HHS Public Access

Author manuscript

Virology. Author manuscript; available in PMC 2017 September 01.

Published in final edited form as:

Virology. 2016 September ; 496: 175–185. doi:10.1016/j.virol.2016.06.004.

The Role of Signal Transducer and Activator of Transcription 3 in Rift Valley Fever Virus Infection

Chelsea Pinkham, **Soyeon An**, **Lindsay Lundberg**, **Neha Bansal**, **Ashwini Benedict**, **Aarthi Narayanan**, and **Kylene Kehn-Hall***

National Center for Biodefense and Infectious Diseases, School of Systems Biology, George Mason University, 10650 Pyramid Place, Manassas, Virginia, United States of America

Abstract

Rift Valley fever (RVF) is a zoonotic disease that can cause severe illness in humans and livestock, triggering spontaneous abortion in almost 100% of pregnant ruminants. In this study, we demonstrate that signal transducer and activator of transcription 3 (STAT3) is phosphorylated on its conserved tyrosine residue (Y705) following RVFV infection. This phosphorylation was dependent on a major virulence factor, the viral nonstructural protein NSs. Loss of STAT3 had little effect on viral replication, but rather resulted in cells being more susceptible to RVFV-induced cell death. Phosphorylated STAT3 translocated to the nucleus, coinciding with inhibition of *fos*, *jun*, and *nr4a2* gene expression, and the presence of STAT3 and NSs at the *nr4a2* promoter. NSs was found predominantly in the cytoplasm of STAT3 null cells, indicating that STAT3 influences NSs nuclear localization. Collectively, these data demonstrate that STAT3 functions in a pro-survival capacity through modulation of NSs localization.

Keywords

Rift Valley fever virus; RVFV; STAT; Signal transducer and activator of transcription; STAT3; NSs; apoptosis; NR4A2

Introduction

First identified in the Rift Valley of Kenya, Rift Valley fever virus (RVFV) is the causative agent of Rift Valley fever (RVF), a mosquito-borne zoonotic disease that can cause severe illness in humans and livestock (Ikegami and Makino, 2011). From the time of its discovery in 1931, RVFV has become endemic to sub-Saharan Africa and has since dispersed to the Arabian Peninsula (Centers for Disease Control and Prevention (CDC), 2000). RVFV outbreaks can have devastating effects on livestock, in which RVFV causes spontaneous abortion in almost 100% of pregnant ruminants, referred to as an “abortion storm,” and high

*Corresponding author. Ph.D., Associate Professor, National Center for Biodefense & Infectious Diseases, School of Systems Biology, George Mason University, Biomedical Research Lab, 10650 Pyramid Place, MS 1J5, Manassas, VA 20110, Tel.: 703-993-8869; Lab: 703-993-9493; fax: 703-993-4280. kkehnhal@gmu.edu.

mortality in young animals (Pepin et al., 2010). Humans can also become infected with RVFV through various routes. Infected mosquitoes play an important role in amplifying the virus and may infect humans through a bite, but humans can also be infected through the handling of infected tissue or fluids. Many cases result in an acute febrile illness with symptoms including chills, dizziness, fever, and headache (Ikegami and Makino, 2011). In a small percentage of cases the disease can progress to severe symptoms including hepatitis, encephalitis, and hemorrhagic fever (Ikegami and Makino, 2011). With the increased risk of spread, competent vectors in many areas of the world, and the ease of international trade and travel, RVFV is considered an overlap select agent by the Centers of Disease Control and Prevention and the U.S. Department of Agriculture (Indran and Ikegami, 2012).

RVFV is a negative sense, single-stranded RNA virus of the family *Bunyaviridae*, genus *Phlebovirus*. The genome encodes three RNA segments termed the S-, M-, and L-segments (Bishop et al., 1980). The S-segment codes for the nucleoprotein, as well as the nonstructural protein NSs in an ambisense fashion (Ikegami and Makino, 2011; Pepin et al., 2010). NSs is of particular interest as it is the major virulence factor of RVFV (Ikegami and Makino, 2004). While RVFV replicates in the cytoplasm, NSs is able to localize to the nucleus where it forms its characteristic filamentous structures (Struthers and Swanepoel, 1982). NSs has various roles during infection, primarily acting as an interferon antagonist by blocking interferon beta (IFN-β) gene expression at the transcriptional level (Billecocq et al., 2004). More specifically, it binds with Sin3A-associated protein (SAP30) and SAP30 co-repressor factors in order to be recruited to the IFN-β promoter to facilitate transcriptional repression (Le May et al., 2008). Additionally, NSs interacts with the p44 subunit of TFIIH, which is sequestered by the characteristic filaments and prevents the assembly of transcription factor II (TFIIH) (Dasgupta, 2004; Le May et al., 2004). NSs also causes degradation of dsRNA-dependent protein kinase (PKR) via the proteasome, which in turn inhibits phosphorylation of eukaryotic translation initiation factor 2α (eIF2α), preventing overall host translational suppression (Billecocq et al., 2004; Habjan et al., 2009; Ikegami et al., 2009). Moreover, NSs interacts with a subunit of the E3 ubiquitin ligase (Kainulainen et al., 2014), which results in the complete degradation of p62 almost immediately after viral entry (Kalveram et al., 2011). Additionally, up-regulation of p53 phosphorylation, as well as other components of the DNA damage pathway, has been observed and is highly dependent on NSs (Austin et al., 2012; Baer et al., 2012). Loss of p53 resulted in lower viral titers and increased cell viability, indicating that p53 is manipulated by the virus in order to replicate more efficiently. It was also shown that cells infected with RVFV MP12 display an S-phase arrest, while the virulent strain ZH548 causes cells to arrest in G_0/G_1, both of which are dependent on NSs (Baer et al., 2012). Overall, NSs is a highly dynamic virulence factor that has a major impact on host cellular functions.

Viruses have evolved to manipulate and regulate host proteins in order to facilitate replication and evade the immune response. Signal transducer and activator of transcription (STAT) proteins are a family of transcription factors that regulate many aspects of the host cell, such as immunity, survival, and proliferation (Bromberg and Darnell Jr., 2000). The Jak-STAT protein cascade is initiated by a variety of external factors, which in turn activates receptor-associated tyrosine kinases (Bromberg and Darnell Jr., 2000). These kinases, such as Janus kinase 2 (Jak2) or tyrosine kinase 2 (Tyk2), proceed to phosphorylate STAT

proteins causing them to assemble into homo- or hetero-dimers and translocate to the nucleus where they associate with co-activators and other transcription factors (Bromberg and Darnell Jr., 2000). STATs can also bind to each other in their unphosphorylated forms, but it is the dimerization of the tyrosine-phosphorylated STATs that allow specific binding to DNA in the nucleus (Reich and Liu, 2006).

STAT3 helps to mediate the expression of various genes in response to external stimuli, such as IL-6 and IL-10. A conventional knockout of STAT3 results in embryonic lethality, which emphasizes its role in growth and development (Takeda et al., 1997). STAT3 is widely studied in the cancer field because of its constitutive activation in many cancers, specifically of the liver (Yu et al., 2009). STAT3 targets include anti-apoptotic genes, such as Bcl-2 and Bcl-xL, as well as genes involved in cell cycle progression, further demonstrating why STAT3 is constitutively phosphorylated in various cancers (Hirano et al., 2000). In contrast, it has recently been shown that STAT3 also suppresses various pro-apoptotic genes in cancer cells, demonstrating its diversity in function (Timofeeva et al., 2013).

The ability of viruses to manipulate the STAT3 pathway has been widely studied in a variety of chronic viral infections. Hepatitis C virus (HCV) core protein interacts and activates STAT3, up-regulates genes such as Bcl-xL and Cyclin D1, promoting cellular transformation (Yoshida et al., 2002). HIV Nef protein triggers a secondary wave of soluble factors, resulting in activation of STAT3 (Percario et al., 2003). A majority of STAT3 studies have focused on cancer and chronic viral infections, signifying the increasing demand to better understand how STAT3 functions in the context of acute infections.

STAT3 is phosphorylated following RVFV infection (Popova et al., 2010), however a detailed analysis of these phosphorylation events and their influence on RVFV has not been determined. Our results show that STAT3 is phosphorylated on the conserved tyrosine residue 705 following RVFV infection. Phosphorylation did not occur following infection with a RVFV strain lacking NSs, indicating that these events take place in a NSs-dependent manner. Further analysis revealed that although STAT3 is not required for RVFV replication, there was an increase in RVFV-induced cell death, revealing a pro-survival role during infection. Of the target genes tested, there was an increase in expression of *nr4a2* in the absence of STAT3 or STAT3 phosphorylation. Furthermore, there was enhanced localization of STAT3 as well as NSs at the promoter of *nr4a2*, indicating that RVFV could be using STAT3 as a means to regulate host gene expression. Finally, NSs was localized predominantly in the cytoplasm of cells lacking STAT3, suggesting that STAT3 plays a role in the nuclear localization of NSs.

Materials and Methods

Cell Culture

Vero cells (ATCC, CCL-81) as well as wild-type mouse embryonic fibroblasts (MEFs) and STAT3 null derivatives were all maintained in Dulbecco's modified minimum essential medium (DMEM) supplemented with 10% fetal bovine serum (FBS), 1% L-glutamine, and 1% penicillin/streptomycin. Human small airway epithelial cells (HSAECs) were acquired from Cambrex Inc., Walkersville, MD and maintained in Ham's F12 medium supplemented

with 10% Fetal Bovine Serum (FBS), 1% L-glutamine, 1% penicillin/streptomycin, 1% nonessential amino acids, 1% sodium pyruvate, 0.001% of 55 mM β-mercaptoethanol. All cell lines were maintained at 37°C with 5% CO_2.

Viruses

Recombinant (r)MP12 virus was rescued and titered as previously described (Benedict et al., 2015). Other recombinant viruses used included the live-attenuated MP12 strain with a complete deletion of the NSs ORF (Ikegami et al., 2006), as well as a strain where a flag tag was added to the C-terminus of NSs (Ikegami et al., 2009). For viral infections, cells were cultured and left to incubate overnight. The next day, cells were infected with the appropriate virus at the specified multiplicity of infection (MOI). Cells were incubated for 1 hour at 37°C and 5% CO_2. Infectious media was removed, washed once with phosphate buffered saline (PBS) without Ca^{2+} and Mg^{2+}, and complete media was added. The cells were left to incubate and collected using the appropriate method for downstream applications at the specified time points.

Western Blot

Protein lysates were collected and analyzed by western blot, or cellular fractionation was performed and analyzed by western blot, as previously described (Austin et al., 2012). In brief, primary antibodies against p-STAT3 Y705 (Cell Signaling, 9145S), total STAT3 (Cell Signaling, 12640S), cleaved Caspase-3 (Cell Signaling, 9661S), Flag (Sigma, F1804), RVFV Nucleoprotein (BEI Resources, NR-43188), Lamin A/C (Cell Signaling, 4777S), GAPDH (Cell Signaling, 5174S), or HRP-conjugated actin (Abcam, ab49900) were diluted in 3% milk solution according to the manufacturer's recommended dilutions followed by the addition of the appropriate secondary antibody.

Immunofluorescence

HSAECs were grown on coverslips in a 6-well plate, infected with MP12-NSs-Flag as described above and fixed for 10 minutes in a solution of 4% paraformaldehyde. Cells were permeabilized, blocked, and probed using primary antibodies against total STAT3 (Cell Signaling, 12640S) and Flag (Sigma, F1804) according to manufacturer's recommendations. After one hour, Alexa Fluor 488 and 568 secondary antibodies were added at a 1:500 dilution in fresh buffer and incubated in the dark for one hour at room temperature. Cells were incubated for 10 minutes in DAPI in PBS in order to visualize the nuclei. After a short PBS wash, cover slips were mounted to glass slides using Fluoromount G and left to dry overnight. Slides were imaged using an oil-immersion 60X objective lens on a Nikon Eclipse TE 2000-U microscope, with all samples subjected to four-line averaging. At least three images were taken of each sample, with one representative image shown. The resulting images were processed through Nikon NIS-Elements AR Analysis 3.2 software. Digitized images were analyzed using the ImageJ version 1.47 public domain software (NIH) to determine the ratio of nuclear (Fn) to cytoplasmic (Fc) fluorescence (Fn/c) according to the formula: $Fn/c = (Fn - Fb)/(Fc - Fb)$, where Fb is background autofluorescence.

Treatments

Human IL-6 was purchased from Cell Signaling (8904SC), and cells were treated with 100 ng/mL of IL-6 for 30 minutes based on an optimization time course in which 30 minutes had the strongest phosphorylation of STAT3 at this concentration.

Cell Viability Assays

Cells were plated in a white-walled 96-well plate and allowed to incubate at 37°C and 5% CO_2 overnight. MEFs were mock-infected or infected with MP12 at the indicated MOI for one hour, then infectious media was washed off and replaced with complete media. At the appropriate time points, all cells were analyzed using CellTiter-Glo Cell Luminescent Viability Assay (Promega, G7570) according to the manufacturer's protocol and as previously described (Lundberg et al., 2013).

Plaque Assay

Cells were plated in a 96-well plate and allowed to incubate overnight at 37°C and 5% CO_2. The next day, infections were performed with MP12 as described above. Supernatants were collected at the indicated time points and stored at −80°C until use. Viral titers were determined by plaque assay as previously described (Baer and Kehn-Hall, 2014).

Transfections

For siRNA transfections, HSAECs were transfected with FlexiTube siRNA directed against STAT3 (Qiagen, SI02662338) or a negative control siRNA. All transfections were done using DharmaFECT 1 transfection reagent (Thermo Scientific, T-2001–02) in Opti-MEM reduced serum medium (Life Technologies, 31985-070). After 24 hours post transfection, transfection media was replaced with fresh Opti-MEM and cultured for an additional 24 hours before infection. The supernatants and protein lysates were collected 24 hpi (72 hours post transfection). The viral titers in the supernatants were determined by plaque assay, while the protein lysates were analyzed by western blot. For DNA transfections, Vero cells were transfected with 2.5 μg of a pI.18-RVFV-NSs-Flag plasmid expressing NSs with a C-terminal Flag-tag or pcDNA as a control using Attractene transfection reagent (Qiagen, 301005). At 24 hours post transfection, cells were lysed and analyzed by western blot for protein expression.

qRT-PCR

Cells were plated in a 12-well plate and mock-infected or infected with RVFV MP12 or MP12-ΔNSs. Cells were collected and RNA was extracted as previously described (Austin et al., 2012) using a RNeasy Mini Kit (Qiagen, 74104) and DNase treated using DNase I (Life Technologies, AM2222) according to manufacturer's protocol. Following DNase treatment, RNA was reverse transcribed into cDNA using a High Capacity RNA-to-cDNA kit with 1–2 μg of RNA (Applied Biosystems, 4387406). Real-time quantitative PCR (qRT-PCR) was performed using the StepOnePlus™ Real-Time PCR System (Life Technologies). TaqMan Gene Expression Assays were used for *fos* (Mm00487425_m1), *jun* (Mm00495062_s1), *nr4a2* (Mm00443060_m1), and *ddit3* (Mm01135937_g1). Fold changes

were calculated relative to 18S ribosomal RNA and normalized to mock samples using the ΔΔCt method.

Chromatin Immunoprecipitation

Cells were cross-linked using 1% paraformaldehyde for 10 minutes at 37°C followed by the addition of glycine to quench the reaction. Chromatin fragments were prepared using 5×10^6 cells per sample, where cells were lysed with SDS lysis buffer (1% SDS, 10 mM EDTA, and 50 mM Tris-HCl pH 8.0) on ice for 10 minutes. Extracts were sonicated on ice in 10 bursts of 20 seconds, then clarified by centrifugation. Sonicated cell supernatant was diluted 10 fold in ChIP dilution buffer (0.01% SDS, 1.1% Triton X-100, 1.2 mM EDTA, 16.7 mM Tris-HC;l pH 8.1, 167 mM NaCl). Immunoprecipitation was performed using Dynabeads® Protein G beads (Thermo Fisher Scientific, 10004D) prepared according to manufacturer's protocol. Primary antibodies were incubated with the beads at room temperature for 20 minutes, washed once, and then incubated with lysates for 2 hours at room temperature. Complexes were washed once with low salt wash buffer (0.1% SDS, 1% Triton X-100, 2 mM EDTA, 20 mM Tris-HCl, pH 8.0, 150 mM NaCl), twice with high salt wash buffer (0.1% SDS, 1% Triton X-100 2 mM EDTA, 20 mM Tris-HCl, pH 8.0, 500 mM NaCl), once with lithium chloride wash buffer (0.25 M LiCl, 1% NP-40, 1% deoxycholate, 1 mM EDTA, 10 mM Tris-HCl, pH 8.0), and once with TE buffer. Complexes were eluted twice with elution buffer (1% SDS, 0.1 M $NaHCO_3$) at room temperature for 15 minutes. NaCl (5 M) was added to the combined elutes and input samples, and incubated at 65°C overnight in order to reverse cross-links. The next day, Proteinase K was added at a final concentration of 50 μg/mL and incubated at 56°C for one hour. The resulting DNA was purified using the ChIP DNA Clean & Concentrator™ (Zymo Research, D5205) according to manufacturer's instructions. Quantitative PCR was performed using SYBR Green PCR Master Mix (Applied Biosystems, 4309155) with 5 μL of immunoprecipitated material and 0.2 μM of primer (nr4a2 forward 5'-TGT CTG CCC GAC CTA CTT TT-3', nr4a2 reverse 5'-ACA GAA ACG CCT GAA GAT GGA-3'). Primers were designed to amplify the predicted STAT3 consensus binding sequence identified 69-tgggTTCCaggactcacca-79 using Genomatix MatInspector Software. Primary antibodies used were V5-tag (ABD Serotec, MCA1360), total STAT3 (Cell Signaling, 12640S), Flag (Sigma, F1804), Tri-Methyl-Histone H3 (Lys4) (H3K4Me, Cell Signaling, 9751), and Di/Tri-Methyl-Histone H3 (Lys9) (H3K9Me, Cell Signaling, 5327).

Statistics

Unless otherwise noted, all statistical analysis was calculated using an unpaired, two-tailed student t-test using Graphpad's QuickCalcs software.

Results

STAT3 is phosphorylated on conserved tyrosine residue 705 in various cell types following RVFV infection

Reverse-phase protein array technology was previously used to identify host signaling pathways that were induced during RVFV infection (Popova et al., 2010). In this study, STAT3 was shown to be phosphorylated following infection, prompting further exploration

into STAT3 and how it is altered by infection. As described previously, NSs is a major virulence factor of RVFV and affects multiple host cell functions (Bouloy and Weber, 2010; Ikegami and Makino, 2011; Pepin et al., 2010). To confirm the previously published results and to determine if this activation is dependent on the viral NSs protein, western blot analysis was performed. Three different cell lines, monkey kidney epithelial cells (Vero cells), human small airway epithelial cells (HSAECs), and mouse embryonic fibroblasts (MEFs) were tested for STAT3 tyrosine phosphorylation on residue 705 (p-STAT3 Y705). Vero cells, HSAECs, and MEFs were mock-infected or infected with the attenuated MP12 strain or the MP12-ΔNSs strain containing a complete deletion of the NSs ORF (Figure 1A). In all cell types infected with RVFV MP12, there was no detectable p-STAT3 Y705 at 4 hours (data not shown and Supplemental Figure 1A) and phosphorylation occurred as early as 8 hpi, being most prominent at 16 hpi. Interestingly, the RVFV-induced signaling is a later event as compared to the classical rapid response due to cytokine induction, which is prominent as early as 15 minutes after treatment with interleukin-6 (IL-6) (Supplemental Figure 1B) (Sin et al., 2012). In HSAECs and MEFs, there was a decrease in STAT3 Y705 phosphorylation at the 24 hour time point which could be the result of a negative feedback loop that may be absent in the Vero cells, due to their impaired immune and inflammatory response (Emeny and Morgan, 1979). Similar increases in phosphorylation of STAT3 was also observed in HepG2 cells (data not shown), despite the constitutive phosphorylation which is common in liver cancer cell lines (Bromberg et al., 1999). These data demonstrate that the increased STAT3 phosphorylation is consistent across different cell types and occurs in human, non-human primate, and mouse cells.

Infection with MP12-ΔNSs resulted in little to no phosphorylation of STAT3. Vero cells are a common cell line used to propagate virus, due to a mutation in the interferon-β (IFN-β) gene that makes cells unable to secrete IFN-α or IFN-β following an infection (Emeny and Morgan, 1979). Nucleoprotein (NP) levels were similar for both MP12 and MP12-ΔNSs viruses in Vero cells (Figure 1A), indicating that the lack of phosphorylation observed with MP12-ΔNSs infection is not due to differing replication rates. However, MP12 and MP12-ΔNSs had differing expression of NP in HSAECS, and even more dramatically different expression of NP in MEFs, suggesting that MP12-ΔNSs has altered replication kinetics in these cells. Taken together, these results indicate that enhanced STAT3 phosphorylation is linked to NSs, can occur independently of type I-interferons, and is a later event, as compared to classical cytokine-induced STAT3 phosphorylation.

To further elucidate whether phosphorylation of STAT3 was directly dependent on NSs, cells were transfected with a plasmid encoding for flag-tagged RVFV NSs or pcDNA as a control. Varying concentrations of plasmid DNA were used and cells collected to determine which concentration provided the best expression of NSs (data not shown). Cells collected at 24 hours post transfection gave the most robust expression of NSs, particularly at the 2.5 μg concentration (Figure 1B). Western blot analysis showed that STAT3 phosphorylation is dependent on NSs, as seen by a significant increase in phosphorylation over the control. These data indicate that expression of NSs is sufficient for STAT3 phosphorylation.

STAT3 localization in RVFV infected cells

Following phosphorylation, the canonical pathway of STAT3 is to translocate to the nucleus and regulate gene expression (Bromberg et al., 1999). Therefore, the distribution of STAT3 following RVFV infection was assessed by confocal microscopy. Both mock-infected and RVFV MP12-infected MEFs showed a predominantly cytoplasmic distribution of STAT3 (Figure 2A). In order to gather information specifically about p-STAT3 (Y705), cellular fractionation was performed to measure the amount of STAT3 in the nuclear and cytoplasmic compartments. As expected, at 16 hpi there was a small amount of constitutive STAT3 phosphorylation in the mock-infected cells (Figure 2B). There was a significant amount of phosphorylated STAT3 in infected cells, with a majority of phosphorylated STAT3 in the nuclear fraction, indicating that phosphorylated STAT3 is able to translocate to the nucleus after infection. As a control, translocation of phosphorylated STAT3 was also tested in the presence of IL-6, a known activator of this pathway. The majority of phosphorylated STAT3 was also detected in the nucleus after IL-6 treatment (Figure 2C). Interestingly, phosphorylated STAT3 was found in both the nuclear and cytoplasmic compartments following RVFV infection of HSAECs (Supplemental Figure 2), indicating that there are some cell specific differences in STAT3 localization. These data indicate that following RVFV infection, phosphorylated STAT3 is found in the nucleus of infected cells.

Loss of STAT3 does not alter RVFV replication kinetics

WT and STAT3 −/− MEFs were analyzed to investigate whether the loss of STAT3 had any effect on RVFV replication. RVFV NP production and viral titers were analyzed at 4, 8, 16 and 24 hpi. Little to no difference in RVFV NP expression was observed in WT MEFs and STAT3 −/− MEFs at either MOI (Figure 3A). Likewise, no significant difference in viral replication kinetics was observed between WT and STAT3 −/− MEFs at either MOI (Figure 3B). In order to confirm these data in a human cell line, HSAECs were utilized for siRNA experiments. To optimize efficient siRNA knockdown, HSAECs were transfected with 10 nM, 25 nM, and 50 nM of siRNA against STAT3 or a negative control siRNA for 48 hours. STAT3 protein expression was significantly decreased at all concentrations tested (Figure 3C). Further experiments were carried out using 25 nM of STAT3 siRNA, which limited the amount of siRNA used, while ensuring efficient knockdown through the course of infection. Next, the effect of STAT3 knock down on RVFV titers was assessed. These data revealed that there was no difference in viral titers following STAT3 knockdown at 8 hpi (Figure 3D). At 16hpi, there was a minor, but statistically significant reduction in viral titers. Even though this reduction is statistically significant, the decrease is not significant enough to suggest that STAT3 is required for viral replication. In summary, these data show that STAT3 is not required for efficient RVFV replication.

Reduction or loss of STAT3 increases RVFV-induced cell death

STAT3 target genes are involved in many processes including immunity, survival, and proliferation (Hirano et al., 2000; Wang et al., 2011; Yoshida et al., 2002). There is increasing evidence that STATs play a role in apoptosis, given that the inhibition of STAT3 induces apoptosis in various cancer cell lines (Aoki et al., 2003; Battle and Frank, 2002; Epling-Burnette et al., 2001). Therefore, the influence of STAT3 on cell survival following

RVFV infection was examined. Cell survival was analyzed by CellTiter-Glo at 24 hpi to determine the effects of STAT3 on host cell survival. At 24 hpi, MP12 caused a 20% decrease in cell viability when compared to the mock-infected cells (Figure 4A). In contrast, STAT3 −/− MEFs had a 40% reduction in cell viability, showing an increase in RVFV-induced cell death. In addition, there was only a slight decrease in cell viability when both cell types were infected with the virus lacking NSs. To confirm these results, western blot analysis of cleaved caspase-3 was performed. In cells lacking STAT3, there was increased expression of cleaved caspase-3 at both MOIs when compared to the control (Figure 4B). These data demonstrate that a lack of STAT3 increases RVFV-induced cell death, indicating that STAT3 plays a pro-survival role during RVFV infection.

Loss of STAT3 leads to an increase in pro-apoptotic gene expression

In its traditional role, tyrosine phosphorylated STAT3 forms dimers and can then translocate to the nucleus where it induces expression of STAT3 responsive genes (Hirano et al., 2000). Recently, it has been established that STAT3 suppresses various pro-apoptotic genes in cancer cells, advancing cell proliferation and reducing apoptosis (Bossy-Wetzel et al., 1997; Timofeeva et al., 2013; Wisdom et al., 1999). Given that previous data showed a lack of STAT3 enhanced RVFV-induced cell death, this hypothesis was investigated further. Four targets of STAT3 were examined, all with roles in cell survival and apoptosis. qRT-PCR analysis revealed that *fos*, *jun*, and *nr4a2* all exhibited increased gene expression at 24 hpi in cells that lacked STAT3 when compared to WT MEFs (Figure 5A). In contrast, *ddit3* did not significantly change following RVFV infection, which was also true following STAT3 inhibition in cancer cells (Timofeeva et al., 2013). These genes were also suppressed in HSAECs infected with RVFV MP12, but had increased expression in cells infected with the MP12-ΔNSs strain which does not induce tyrosine phosphorylation of STAT3 (data not shown). In brief, these data indicate that expression of pro-apoptotic genes, such as the ones tested here, are suppressed following RVFV infection in an STAT3 dependent manner. In contrast, these genes are significantly increased following RVFV infection in cells lacking STAT3, providing one explanation for cells lacking STAT3 having a higher level of RVFV-induced cell death following infection.

STAT3 and NSs are present at the *nr4a2* promoter

The previous results indicated that in the absence of STAT3, pro-apoptotic gene expression is increased in RVFV-infected cells. While *fos* is widely studied in multiple diseases as well as its role in apoptosis, the nuclear receptor family of intracellular transcription factors is understudied, especially in the context of acute infection. Furthermore, a previous study identified NSs as interacting with the *nr4a2* promoter through chromatin immunoprecipitation coupled with DNA microarray (ChIP-chip) analysis, prompting further examination of this particular gene (Benferhat et al., 2012). To determine if the observed STAT3 effects are due to a direct interaction of STAT3 with the *nr4a2* promoter, ChIP was performed. Genomatix MatInspector software was used to determine the predicted STAT3 binding site for the *nr4a2* promoter. Only one STAT3 binding site was predicted at positions 61–79 and PCR primers were designed to assess this area of interest. ChIP analysis revealed that STAT3 presence was significantly increased at the *nr4a2* promoter in WT cells following infection (Figure 5B). Interestingly, these results also indicated that there was an

increased presence of NSs at the promoter region of *nr4a2*. In cells lacking STAT3, there was little to no NSs present, which may indicate that STAT3 is necessary for the recruitment of NSs to the promoter. Two lysine methylated histones were also tested, in which lysine methylation on residue 4 of histone H3 (H3K4Me3) is a marker of active gene expression, while lysine methylation on residue 9 of histone H3 (H3K9Me3) is associated more with genes that are inactive (Barski et al., 2007; Nguyen et al., 2002; Santos-Rosa et al., 2002; Stewart et al., 2005). H3K4Me3 expression at the promoter of *nr4a2* had almost a 3-fold increase in cells lacking STAT3 (Figure 5C). Conversely, H3K9Me3 expression was decreased in STAT3 −/− cells when compared to WT MEFs. These results correspond to the enhancement of *nr4a2* gene expression observed in the absence of STAT3 (Figure 5A). These results suggest that the presence of STAT3 and NSs at the promoter of *nr4a2* during RVFV infection suppresses *nr4a2* gene expression.

Loss of STAT3 alters NSs localization and filament formation in the nucleus of infected cells

During infection, NSs suppresses general host transcription by sequestering TFIIH subunits, inducing the degradation of TFIIH p62, and binding to chromatin remodeling proteins (Dasgupta, 2004; Le May et al., 2004; Le May et al., 2008; Ikegami et al., 2011; Kainulainen et al., 2014). Knowing that these events occur in RVFV-infected cells, the increases in gene expression seen in Figure 5 were unexpected, given that many host genes are suppressed by NSs. To further elucidate this mechanism, the localization of RVFV NSs was analyzed in WT and STAT3 −/− MEFs. Cells were infected with MP12-NSs-Flag and analyzed by confocal microscopy. WT MEFs displayed the characteristic filaments in the nucleus of infected cells with about 85% of cells staining positive for NSs at 24 hpi (Figure 6A and 6B). In contrast, while a similar percentage of STAT3 −/− MEFs were infected at 24 hpi, NSs was localized mainly in the cytoplasm with only a small amount of filament formation. Similar amounts of NSs were present in both WT and STAT3 −/− MEFs at 24 hpi, while cells collected at 16 hpi showed a statistically significant increase in the expression of NSs in STAT3 −/− MEFs (Figure 6B).

To quantitate NSs localization, the nuclear to cytoplasmic fluorescence ratio (Fn/c) was measured and the % of filament containing cells calculated (Figure 6C). An Fn/c value greater than one denotes predominately nuclear fluorescence, whereas a score below one indicates cytoplasmic fluorescence. The nuclear and cytoplasmic distribution of NSs was significantly altered, revealing that NSs was mainly nuclear in WT MEFs while NSs remained predominantly cytoplasmic in STAT3 −/− MEFs cells (Figure 6C, left panel). In agreement with these results, at 24 hpi, almost 60% of infected WT MEFs displayed filament formation, while less than 10% of infected STAT3 −/− MEFs exhibited nuclear filaments (Figure 6C, right panel). Importantly, the differences in NSs localization and filament formation corresponded to the increased gene expression observed in STAT3 −/− MEFs at 24 hpi. These data suggest that STAT3 is influencing NSs' nuclear localization and filament formation.

Discussion

STAT3 has numerous functions in the cell and could be exploited for any number of reasons in order to provide a more ideal environment for viral replication. STAT3 is activated by some viruses in order to promote cell survival, and in the case of Hepatitis B virus (HBV) and Hepatitis C virus (HCV), proliferation and transformation (Lee and Yun, 1998, p. 3; Yoshida et al., 2002, p. 3). Hepatitis B virus (HBV) enhances STAT3 and STAT5 phosphorylation, as well as STAT binding and transcriptional activity through the X-gene product (HBx) (Lee and Yun, 1998). In the context of HCV, STAT3 activation is widely examined due to its role in cell growth. One study indicated that HCV core protein activates STAT3 on its tyrosine residue, which results in rapid proliferation and cellular transformation (Yoshida et al., 2002). Conversely, another study demonstrated that STAT3 is activated by the complex formed by viral protein NS5A and JAK1, resulting in translocation to the nucleus (Sarcar et al., 2004). A subsequent study that showed HCV induces production of reactive oxygen species, consequently leading to DNA damage and activation of STAT3 (Machida et al., 2006). The cause of STAT3 activation has been debated in HBV and HCV, reinforcing the complexity of STAT3 and its function in viral infections, as well as its ability to modulate host gene expression.

Popova et al. indicated that phosphorylation of STAT1 and STAT3 were increased following infection with RVFV (Popova et al., 2010). Here we expanded on these observations to elucidate the role of STAT3 in RVFV infection. STAT3 phosphorylation, specifically of the conserved tyrosine residue (705), exhibited the most dramatic change and was increased after infection with the MP12 strain predominately at 16 hpi. Not only was phosphorylation enhanced following infection, but this phosphorylation was minimal with the RVFV strain containing a deletion of NSs. This event was further confirmed by transfecting in the NSs protein independent of the virus, which still resulted in a significant increase in STAT3 phosphorylation. STAT3 phosphorylation was also observed following infection with the fully virulent strain of RVFV, ZH548 (data not shown), which indicates that these data are not just limited to the live-attenuated strain, MP12. RVFV induced phosphorylation of STAT3 occurred in a delayed fashion, compared to classical cytokine-induced STAT3 stimulation. STAT3 phosphorylation was also observed in interferon deficient Vero cells, further substantiating its independence from the initial type I interferon response, although activation by type II and III interferons could still be possible. Our results also revealed that phosphorylated STAT3 was present in the nucleus of infected MEFs; whereas phosphorylated STAT3 was found in both the cytoplasm and nucleus of infected HSAECS, indicating cell specific effects. STAT3 can be activated by other cytokines such as granulocyte colony-stimulating factor (GCSF), epidermal growth factor (EGF), and other interleukins like IL-2 and IL-10 (Qi and Yang, 2014; Munoz et al., 2014). Also, depending on the stimuli, STAT3 can form heterodimers with STAT1, STAT4, and STAT5 (Delgoffe and Vignali, 2013). Here, IL-6 was chosen as a control since this activation pathway has been heavily studied. IL-6 treatment of both MEFs and HSAECs resulted in phosphorylated STAT3 being predominantly in the nucleus.

There are numerous studies indicating that STAT3 activates expression of multiple genes, particularly in cancers and chronic viral infections, but the suppression of gene expression

by STAT3 remains largely elusive. Additionally, the modulation of STAT3 is mostly understudied, especially in the context of acute viral infections. After confirming that phosphorylated STAT3 was translocating into the nucleus of infected cells, we tested multiple genes that could potentially be modulated by STAT3. Nuclear receptor subfamily 4, group A, member 2 (NR4A2), also known as nuclear receptor related 1 protein (Nurr1), is part of the NR4A family of nuclear receptors. This transcriptional regulator is mostly studied in the context of neurological phenotypes and disorders, such as Parkinson's disease, drug addiction, schizophrenia, and manic depressive disorder (Buervenich et al., 2000; Johnson et al., 2011). While there are no direct pro-apoptotic effects reported for NR4A2, a previous study indicated that NR4A2 acts as a pro-apoptotic gene by functional clustering (Timofeeva et al., 2013), and other members of the nuclear hormone receptor superfamily have been shown to have pro-apoptotic effects (Li et al., 2006). NR4A1 increases T cell receptor-dependent apoptosis, and can also act as a transcription factor in order to target genes that are responsible for apoptosis (Li et al., 2006). NR4A3 has also been shown to be functionally redundant, as it also causes T-cell dependent apoptosis (Cheng et al., 1997). Therefore, it is possible that NR4A2 may have pro-apoptotic effects that have yet to be revealed. Fos, a proto-oncogene, has also been implicated in a pro-apoptotic role, which has been widely studied in the context of cancer and cellular transformation. Fos dimerizes with the Jun family of proteins in order to form the transcription factor activator protein-1 (AP-1) (Shaulian and Karin, 2002). Evidence for pro-apoptotic and pro-survival roles of AP-1 have been reported, as well as speculation of protective activity through STAT3 (Ameyar et al., 2003; Shaulian and Karin, 2002). Additionally, DNA-damage-inducible transcript 3 (DDIT3), also known as CHOP, is another transcription factor known for its role in apoptosis, in which DDIT3 is activated due to cellular stress and in turn promotes apoptosis (Jauhiainen et al., 2012; Laybutt et al., 2007). Each of these genes has a dynamic role in apoptosis, and could be working with STAT3 to play a role in viral-induced apoptosis. Out of the four genes tested, *fos*, *nr4a2*, and *ddit3* all contained predicted STAT3 binding sites in their promoters. Conversely, there was no predicted binding site for STAT3 in the *jun* promoter region. While STAT3 has been shown to interact with c-Jun to regulate transcription, it is unlikely that STAT3 is directly regulating the gene expression of *jun* (Zhang et al., 1999). A recent study showed that STAT3 inhibition resulted in enhanced expression of multiple genes that had pro-apoptotic functions, and that loss-of-function studies of any one gene was not enough to overcome the induction of apoptosis by other genes (Timofeeva et al., 2013). Therefore, the increased induction of apoptosis in cells lacking STAT3 could be quite complex, as multiple pathways would come into play in the regulation of apoptosis.

Our data indicated that STAT3 and NSs are present at the *nr4a2* promoter region. NSs has previously been detected at the IFN-β promoter (Le May et al., 2008) and bound to pericentromeric DNA (Mansuroglu et al., 2010). The interaction of NSs with promoters was also studied on a global scale using the ChIP-on-chip technique (Benferhat et al., 2012). Supplemental data from this publication indicated that NSs was present at the promoter of *nr4a2* and *fosl2*, a fos family member. There is no evidence indicating that NSs interacts directly with cellular DNA, rather it is likely that NSs is recruited to promoters through interaction with transcription factors or chromatin remodeling proteins. However, we were

unable to detect an interaction between NSs and STAT3 (data not shown), suggesting that these two proteins do not interact directly. Rather, it is likely that they are part of either a large complex or in distinct complexes at the *nr4a2* promoter.

Further analysis revealed that there was an alteration in localization of NSs in cells that lacked STAT3. In these cells, NSs was predominantly cytoplasmic when compared to the WT MEFs, which showed a nuclear accumulation of NSs as well as the characteristic filaments. In STAT3−/− MEFs IFN-β gene expression was increased, but the ability of NSs to induce degradation of PKR was retained (data not shown), indicating that the cytoplasmic function of NSs is retained in STAT3 −/− MEFs. In addition, these results suggest that STAT3 is having an indirect effect on NSs localization and filament formation. One possibility is that a transcriptional target of STAT3 is needed for the nuclear importation of NSs. Further studies are needed to determine the precise mechanism by which STAT3 and/or STAT3 transcriptional targets affect NSs localization.

The current study suggests a novel relationship of STAT3 regulation of *nr4a2* in the context of RVFV infection. Overall, our data suggest that the phosphorylation of STAT3 in RVFV infection results in translocation of STAT3 into the nucleus in order to suppress pro-apoptotic gene expression. The results indicated that both viral protein NSs and STAT3 had an increased presence at the promoter of *nr4a2* in WT cells, indicating that RVFV may utilize STAT3 in order to regulate expression of apoptotic genes. The absence of STAT3 and corresponding cytoplasmic localization of NSs allows for increased pro-apoptotic gene expression, which is supported by the increase in RVFV-induced apoptosis in cells lacking STAT3. This study highlights another complex role of STAT3, especially in the context of an acute viral infection, which is largely understudied. These data also deepen the understanding of the complex functional roles of STAT3, as well as the mechanisms by which RVFV helps to suppress host cell apoptotic signals in order to survive.

Supplementary Material

Refer to Web version on PubMed Central for supplementary material.

Acknowledgments

The authors thank Dr. David Levy (New York University) and Dr. Stephanie Watowich (University of Texas, MD Anderson Cancer Center) for providing the STAT3 −/− MEF cells, as well as Dr. Ursula Buchholz for the BSR-T7/5 cell line to generate the MP12 virus. The authors also thank Dr. Shinji Makino (University of Texas Medical Branch) for MP12-ΔNSs, MP12-NSs-Flag, and the MP12 reverse genetics system. The RVFV nucleoprotein antibody used in these experiments were a kind gift from Dr. Connie Schmaljohn (USAMRIID). The authors also thank Dr. Friedemann Weber (University of Freiburg) for the NSs-Flag plasmid. Finally, thank you to Dr. Cynthia de la Fuente (George Mason University) for helpful discussions and edits. This work was supported through the NIH research grant 1R15AI100001-01A1 to KK. This material is based upon work supported by the U.S. Department of Homeland Security under Cooperative Agreement Number DHS 2010-ST-061-AG0002 (Institute for Infectious Animal Diseases (IIAD) Fellowship to AB). The views and conclusions contained in this document are those of the authors and should not be interpreted as necessarily representing the official polices, either expressed or implied, of the U.S. Department of Homeland Security.

References

Ameyar M, Wisniewska M, Weitzman JB. A role for AP-1 in apoptosis: the case for and against. Biochimie, Apoptosis: from regulation to infection. Protein phosphatase “Eminence grise of Apoptosis” web site: http://pp1signature.pasteur.fr. 2003; 85:747–752.

Aoki Y, Feldman GM, Tosato G. Inhibition of STAT3 signaling induces apoptosis and decreases survivin expression in primary effusion lymphoma. Blood. 2003; 101:1535–1542. [PubMed: 12393476]

Austin D, Baer A, Lundberg L, Shafagati N, Schoonmaker A, Narayanan A, Popova T, Panthier JJ, Kashanchi F, Bailey C, Kehn-Hall K. p53 Activation following Rift Valley Fever Virus Infection Contributes to Cell Death and Viral Production. PLoS ONE. 2012; 7:e36327. [PubMed: 22574148]

Baer A, Austin D, Narayanan A, Popova T, Kainulainen M, Bailey C, Kashanchi F, Weber F, Kehn-Hall K. Induction of DNA damage signaling upon Rift Valley fever virus infection results in cell cycle arrest and increased viral replication. J. Biol. Chem. 2012; 287:7399–7410. [PubMed: 22223653]

Baer A, Kehn-Hall K. Viral concentration determination through plaque assays: using traditional and novel overlay systems. J. Vis. Exp. JoVE. 2014:e52065. [PubMed: 25407402]

Barski A, Cuddapah S, Cui K, Roh T-Y, Schones DE, Wang Z, Wei G, Chepelev I, Zhao K. High-resolution profiling of histone methylations in the human genome. Cell. 2007; 129:823–837. [PubMed: 17512414]

Battle TE, Frank DA. The Role of STATs in Apoptosis. Curr. Mol. Med. 2002; 2:381–392. [PubMed: 12108949]

Benedict A, Bansal N, Senina S, Hooper I, Lundberg L, de la Fuente C, Narayanan A, Gutting B, Kehn-Hall K. Repurposing FDA-approved drugs as therapeutics to treat Rift Valley fever virus infection. Virology. 2015; 6:676.

Benferhat R, Josse T, Albaud B, Gentien D, Mansuroglu Z, Marcato V, Souès S, Le Bonniec B, Bouloy M, Bonnefoy E. Large-scale chromatin immunoprecipitation with promoter sequence microarray analysis of the interaction of the NSs protein of Rift Valley fever virus with regulatory DNA regions of the host genome. J. Virol. 2012; 86:11333–11344. [PubMed: 22896612]

Billecocq A, Spiegel M, Vialat P, Kohl A, Weber F, Bouloy M, Haller O. NSs protein of Rift Valley fever virus blocks interferon production by inhibiting host gene transcription. J. Virol. 2004; 78:9798–9806. [PubMed: 15331713]

Bishop DH, Calisher CH, Casals J, Chumakov MP, Gaidamovich SY, Hannoun C, Lvov DK, Marshall ID, Oker-Blom N, Pettersson RF, Porterfield JS, Russell PK, Shope RE, Westaway EG. Bunyaviridae. Intervirology. 1980; 14:125–143. [PubMed: 6165702]

Bossy-Wetzel E, Bakiri L, Yaniv M. Induction of apoptosis by the transcription factor c-Jun. EMBO J. 1997; 16:1695–1709. [PubMed: 9130714]

Bouloy M, Weber F. Molecular biology of rift valley Fever virus. Open Virol. J. 2010; 4:8–14. [PubMed: 20517489]

Bromberg J, Darnell J Jr. The role of STATs in transcriptional control and their impact on cellular function. Publ. Online 22 May 2000 Doi101038sjonc1203476. 2000; 19

Bromberg JF, Wrzeszczynska MH, Devgan G, Zhao Y, Pestell RG, Albanese C, Darnell JE Jr. Stat3 as an Oncogene. Cell. 1999; 98:295–303. [PubMed: 10458605]

Buervenich S, Carmine A, Arvidsson M, Xiang F, Zhang Z, Sydow O, Jönsson EG, Sedvall GC, Leonard S, Ross RG, Freedman R, Chowdari KV, Nimgaonkar VL, Perlmann T, Anvret M, Olson L. NURR1 Mutations in cases of schizophrenia and manic-depressive disorder. Am. J. Med. Genet. 2000; 96:808–813. [PubMed: 11121187]

Centers for Disease Control and Prevention (CDC). Outbreak of Rift Valley fever--Saudi Arabia, August-October, 2000. MMWR Morb. Mortal. Wkly. Rep. 2000; 49:905–908. [PubMed: 11043643]

Cheng LE, Chan FK, Cado D, Winoto A. Functional redundancy of the Nur77 and Nor-1 orphan steroid receptors in T-cell apoptosis. EMBO J. 1997; 16:1865–1875. [PubMed: 9155013]

Dasgupta A. Targeting TFIIH to inhibit host cell transcription by Rift Valley Fever Virus. Mol. Cell. 2004; 13:456–458. [PubMed: 14992716]

Delgoffe GM, Vignali DAA. STAT heterodimers in immunity: A mixed message or a unique signal? JAK-STAT. 2013; 2(1):e23060. http://doi.org/10.4161/jkst.23060. [PubMed: 24058793]

Emeny JM, Morgan MJ. Regulation of the interferon system: evidence that Vero cells have a genetic defect in interferon production. J. Gen. Virol. 1979; 43:247–252. [PubMed: 113494]

Epling-Burnette PK, Liu JH, Catlett-Falcone R, Turkson J, Oshiro M, Kothapalli R, Li Y, Wang J-M, Yang-Yen H-F, Karras J, Jove R, Loughran TP. Inhibition of STAT3 signaling leads to apoptosis of leukemic large granular lymphocytes and decreased Mcl-1 expression. J. Clin. Invest. 2001; 107:351–362. [PubMed: 11160159]

Habjan M, Pichlmair A, Elliott RM, Overby AK, Glatter T, Gstaiger M, Superti-Furga G, Unger H, Weber F. NSs protein of rift valley fever virus induces the specific degradation of the double-stranded RNA-dependent protein kinase. J. Virol. 2009; 83:4365–4375. [PubMed: 19211744]

Hirano T, Ishihara K, Hibi M. Roles of STAT3 in mediating the cell growth, differentiation and survival signals relayed through the IL-6 family of cytokine receptors. Oncogene. 2000; 19:2548–2556. [PubMed: 10851053]

Huang NE, Lin CH, Lin YS, Yu WCY. Modulation of YY1 activity by SAP30. Biochem. Biophys. Res. Commun. 2003; 306:267–275. [PubMed: 12788099]

Icardi L, Mori R, Gesellchen V, Eyckerman S, De Cauwer L, Verhelst J, Vercauteren K, Saelens X, Meuleman P, Leroux-Roels G, De Bosscher K, Boutros M, Tavernier J. The Sin3a repressor complex is a master regulator of STAT transcriptional activity. Proc. Natl. Acad. Sci. U.S.A. 2012; 109:12058–12063. [PubMed: 22783022]

Ikegami T, Makino S. The pathogenesis of Rift Valley fever. Viruses. 2011; 3:493–519. [PubMed: 21666766]

Ikegami T, Makino S. [Rift Valley fever virus]. Uirusu. 2004; 54:229–235. [PubMed: 15745161]

Ikegami T, Narayanan K, Won S, Kamitani W, Peters CJ, Makino S. Dual functions of Rift Valley fever virus NSs protein: inhibition of host mRNA transcription and post-transcriptional downregulation of protein kinase PKR. Ann. N. Y. Acad. Sci. 2009; 1171(Suppl 1):E75–E85. [PubMed: 19751406]

Ikegami T, Won S, Peters CJ, Makino S. Rescue of Infectious Rift Valley Fever Virus Entirely from cDNA, Analysis of Virus Lacking the NSs Gene, and Expression of a Foreign Gene. J. Virol. 2006; 80:2933–2940. [PubMed: 16501102]

Indran SV, Ikegami T. Novel approaches to develop Rift Valley fever vaccines. Front. Cell. Infect. Microbiol. 2012; 2:131. [PubMed: 23112960]

Jauhiainen A, Thomsen C, Strömbom L, Grundevik P, Andersson C, Danielsson A, Andersson MK, Nerman O, Rörkvist L, Ståhlberg A, Åman P. Distinct Cytoplasmic and Nuclear Functions of the Stress Induced Protein DDIT3/CHOP/GADD153. PLoS ONE. 2012; 7:e33208. [PubMed: 22496745]

Johnson MM, Michelhaugh SK, Bouhamdan M, Schmidt CJ, Bannon MJ. The Transcription Factor NURR1 Exerts Concentration-Dependent Effects on Target Genes Mediating Distinct Biological Processes. Front. Neurosci. 2011; 5

Kainulainen M, Habjan M, Hubel P, Busch L, Lau S, Colinge J, Superti-Furga G, Pichlmair A, Weber F. Virulence factor NSs of Rift Valley fever virus recruits the F-box protein FBXO3 to degrade subunit p62 of general transcription factor TFIIH. J. Virol. 2014

Kalveram B, Lihoradova O, Ikegami T. NSs protein of rift valley fever virus promotes posttranslational downregulation of the TFIIH subunit p62. J. Virol. 2011; 85:6234–6243. [PubMed: 21543505]

Laybutt DR, Preston AM, Åkerfeldt MC, Kench JG, Busch AK, Biankin AV, Biden TJ. Endoplasmic reticulum stress contributes to beta cell apoptosis in type 2 diabetes. Diabetologia. 2007; 50:752–763. [PubMed: 17268797]

Lee Y-H, Yun Y. HBx Protein of Hepatitis B Virus Activates Jak1-STAT Signaling. J. Biol. Chem. 1998; 273:25510–25515. [PubMed: 9738022]

Le May N, Dubaele S, Proietti De Santis L, Billecocq A, Bouloy M, Egly J-M. TFIIH transcription factor, a target for the Rift Valley hemorrhagic fever virus. Cell. 2004; 116:541–550. [PubMed: 14980221]

Le May N, Mansuroglu Z, Léger P, Josse T, Blot G, Billecocq A, Flick R, Jacob Y, Bonnefoy E, Bouloy M. A SAP30 complex inhibits IFN-beta expression in Rift Valley fever virus infected cells. PLoS Pathog. 2008; 4:e13. [PubMed: 18225953]

Li Q-X, Ke N, Sundaram R, Wong-Staal F. NR4A1, 2, 3--an orphan nuclear hormone receptor family involved in cell apoptosis and carcinogenesis. Histol. Histopathol. 2006; 21:533–540. [PubMed: 16493583]

Lundberg L, Pinkham C, Baer A, Amaya M, Narayanan A, Wagstaff KM, Jans DA, Kehn-Hall K. Nuclear import and export inhibitors alter capsid protein distribution in mammalian cells and reduce Venezuelan Equine Encephalitis Virus replication. Antiviral Res. 2013; 100:662–672. [PubMed: 24161512]

MacDonald ML, Lamerdin J, Owens S, Keon BH, Bilter GK, Shang Z, Huang Z, Yu H, Dias J, Minami T, Michnick SW, Westwick JK. Identifying off-target effects and hidden phenotypes of drugs in human cells. Nat. Chem. Biol. 2006; 2:329–337. [PubMed: 16680159]

Machida K, Cheng KT-H, Lai C-K, Jeng K-S, Sung VM-H, Lai MMC. Hepatitis C Virus Triggers Mitochondrial Permeability Transition with Production of Reactive Oxygen Species, Leading to DNA Damage and STAT3 Activation. J. Virol. 2006; 80:7199–7207. [PubMed: 16809325]

Mansuroglu Z, Josse T, Gilleron J, Billecocq A, Leger P, Bouloy M, Bonnefoy E. Nonstructural NSs Protein of Rift Valley Fever Virus Interacts with Pericentromeric DNA Sequences of the Host Cell, Inducing Chromosome Cohesion and Segregation Defects. J. Virol. 2010; 84:928–939. [PubMed: 19889787]

Munoz J, Dhillon N, Janku F, Watowich SS, Hong DS. STAT3 inhibitors: finding a home in lymphoma and leukemia. Oncologist. 2014 May; 19(5):536–544. [PubMed: 24705981]

Nguyen CT, Weisenberger DJ, Velicescu M, Gonzales FA, Lin JCY, Liang G, Jones PA. Histone H3-Lysine 9 Methylation Is Associated with Aberrant Gene Silencing in Cancer Cells and Is Rapidly Reversed by 5-Aza-2′-deoxycytidine. Cancer Res. 2002; 62:6456–6461. [PubMed: 12438235]

Pepin M, Bouloy M, Bird BH, Kemp A, Paweska J. Rift Valley fever virus (Bunyaviridae: Phlebovirus): an update on pathogenesis, molecular epidemiology, vectors, diagnostics and prevention. Vet. Res. 2010; 41

Percario Z, Olivetta E, Fiorucci G, Mangino G, Peretti S, Romeo G, Affabris E, Federico M. Human immunodeficiency virus type 1 (HIV-1) Nef activates STAT3 in primary human monocyte/macrophages through the release of soluble factors: involvement of Nef domains interacting with the cell endocytotic machinery. J. Leukoc. Biol. 2003; 74:821–832. [PubMed: 12960275]

Popova TG, Turell MJ, Espina V, Kehn-Hall K, Kidd J, Narayanan A, Liotta L, Petricoin EF 3rd, Kashanchi F, Bailey C, Popov SG. Reverse-phase phosphoproteome analysis of signaling pathways induced by Rift valley fever virus in human small airway epithelial cells. PloS One. 2010; 5:e13805. [PubMed: 21072193]

Qi QR, Yang ZM. Regulation and function of signal transducer and activator of transcription 3. World J Biol Chem. 2014 May 26; 5(2):231–239. [PubMed: 24921012]

Reich NC, Liu L. Tracking STAT nuclear traffic. Nat. Rev. Immunol. 2006; 6:602–612. [PubMed: 16868551]

Santos-Rosa H, Schneider R, Bannister AJ, Sherriff J, Bernstein BE, Emre NCT, Schreiber SL, Mellor J, Kouzarides T. Active genes are tri-methylated at K4 of histone H3. Nature. 2002; 419:407–411. [PubMed: 12353038]

Sarcar B, Ghosh AK, Steele R, Ray R, Ray RB. Hepatitis C virus NS5A mediated STAT3 activation requires co-operation of Jak1 kinase. Virology. 2004; 322:51–60. [PubMed: 15063116]

Schust J, Sperl B, Hollis A, Mayer TU, Berg T. Stattic: a small-molecule inhibitor of STAT3 activation and dimerization. Chem. Biol. 2006; 13:1235–1242. [PubMed: 17114005]

Sen N, Che X, Rajamani J, Zerboni L, Sung P, Ptacek J, Arvin AM. Signal transducer and activator of transcription 3 (STAT3) and survivin induction by varicella-zoster virus promote replication and skin pathogenesis. Proc. Natl. Acad. Sci. 2012; 109:600–605. [PubMed: 22190485]

Shaulian E, Karin M. AP-1 as a regulator of cell life and death. Nat. Cell Biol. 2002; 4:E131–E136. [PubMed: 11988758]

Sin W-X, Li P, Yeong JP-S, Chin K-C. Activation and regulation of interferon-β in immune responses. Immunol. Res. 2012; 53:25–40. [PubMed: 22411096]

Steegmann JL, Cervantes F, le Coutre P, Porkka K, Saglio G. Off-target effects of BCR–ABL1 inhibitors and their potential long-term implications in patients with chronic myeloid leukemia. Leuk. Lymphoma. 2012; 53:2351–2361. [PubMed: 22616642]

Stewart MD, Li J, Wong J. Relationship between Histone H3 Lysine 9 Methylation, Transcription Repression, and Heterochromatin Protein 1 Recruitment. Mol. Cell. Biol. 2005; 25:2525–2538. [PubMed: 15767660]

Struthers JK, Swanepoel R. Identification of a Major Non-structural Protein in the Nuclei of Rift Valley Fever Virus-infected Cells. J. Gen. Virol. 1982; 60:381–384. [PubMed: 7108491]

Tai AW, Benita Y, Peng LF, Kim S-S, Sakamoto N, Xavier RJ, Chung RT. A Functional Genomic Screen Identifies Cellular Cofactors of Hepatitis C Virus Replication. Cell Host Microbe. 2009; 5:298–307. [PubMed: 19286138]

Takeda K, Noguchi K, Shi W, Tanaka T, Matsumoto M, Yoshida N, Kishimoto T, Akira S. Targeted disruption of the mouse Stat3 gene leads to early embryonic lethality. Proc. Natl. Acad. Sci. 1997; 94:3801–3804. [PubMed: 9108058]

Timofeeva OA, Tarasova NI, Zhang X, Chasovskikh S, Cheema AK, Wang H, Brown ML, Dritschilo A. STAT3 suppresses transcription of proapoptotic genes in cancer cells with the involvement of its N-terminal domain. Proc. Natl. Acad. Sci. U. S. A. 2013; 110:1267–1272. [PubMed: 23288901]

Wang W-B, Levy DE, Lee C-K. STAT3 Negatively Regulates Type I IFN-Mediated Antiviral Response. J. Immunol. 2011; 187:2578–2585. [PubMed: 21810606]

Wauson EM, Guerra ML, Barylko B, Albanesi JP, Cobb MH. Off-Target Effects of MEK Inhibitors. Biochemistry (Mosc.). 2013; 52:5164–5166.

Wisdom R, Johnson RS, Moore C. c-Jun regulates cell cycle progression and apoptosis by distinct mechanisms. EMBO J. 1999; 18:188–197. [PubMed: 9878062]

Yoshida T, Hanada T, Tokuhisa T, Kosai K, Sata M, Kohara M, Yoshimura A. Activation of STAT3 by the hepatitis C virus core protein leads to cellular transformation. J. Exp. Med. 2002; 196:641–653. [PubMed: 12208879]

Yu H, Pardoll D, Jove R. STATs in cancer inflammation and immunity: a leading role for STAT3. Nat. Rev. Cancer. 2009; 9:798–809. [PubMed: 19851315]

Zhang X, Wrzeszczynska MH, Horvath CM, Darnell JE Jr. Interacting regions in Stat3 and c-Jun that participate in cooperative transcriptional activation. Mol Cell Biol. 1999 Oct; 19(10):7138–7146. [PubMed: 10490649]

Zhou Y, Zhao C, Gery S, Braunstein GD, Okamoto R, Alvarez R, Miles SA, Doan NB, Said JW, Gu J, Koeffler HP. Off-Target Effects of c-MET Inhibitors on Thyroid Cancer Cells. Mol. Cancer Ther. 2014; 13:134–143. [PubMed: 24170771]

Highlights

- STAT3 is phosphorylated on tyrosine residue 705 following RVFV infection.
- Phosphorylation of STAT3 was dependent on the viral protein NSs.
- STAT3 −/− MEFs were more susceptible to RVFV-induced cell death.
- Loss of STAT3 led to an increase in pro-apoptotic gene expression.
- STAT3 functions in a pro-survival capacity by modulation of NSs localization.

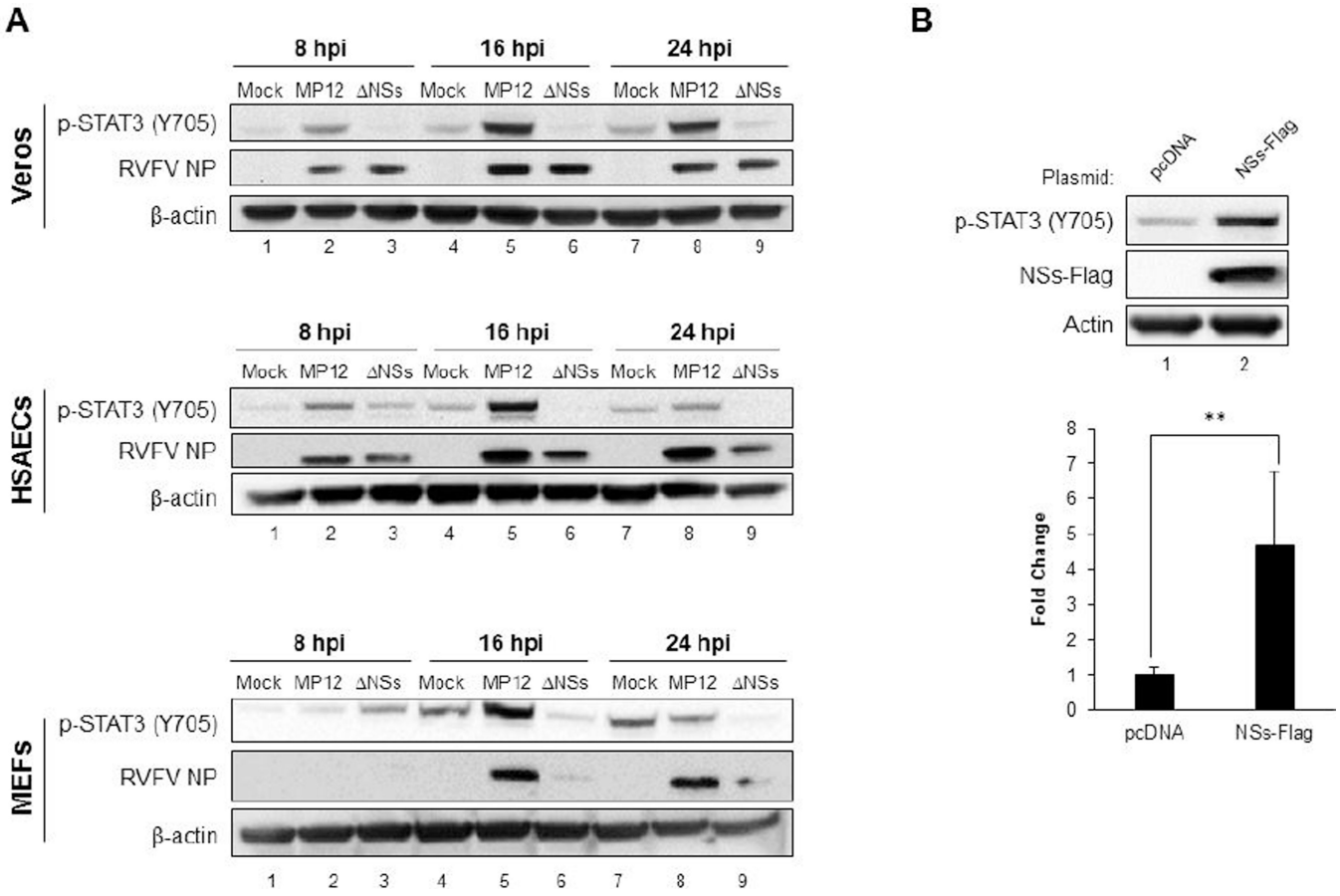

Figure 1. STAT3 is phosphorylated on conserved tyrosine residue 705 in various cell types following RVFV infection

A) Vero, HSAEC, or MEF cells were mock-infected or infected with MP12 or MP12-ΔNSs at MOI 3.0 for one hour. Cell lysates were collected at 8, 16, and 24 hpi and analyzed by western blot. Membranes were probed for p-STAT3 (Y705), RVFV nucleoprotein (NP), and β-actin as a loading control. B) Vero cells were transfected with 2.5 μg of NSs-Flag plasmid or pcDNA as a control. At 24 hours post transfection, cell lysates were collected and analyzed by western blot for p-STAT3 (Y705), RVFV NSs (Flag-tag), and β-actin as a loading control. Blots from two independent experiments (5 biological replicates) were quantified for p-STAT3 (Y705) and a representative blot is shown. ** $p \leq 0.005$

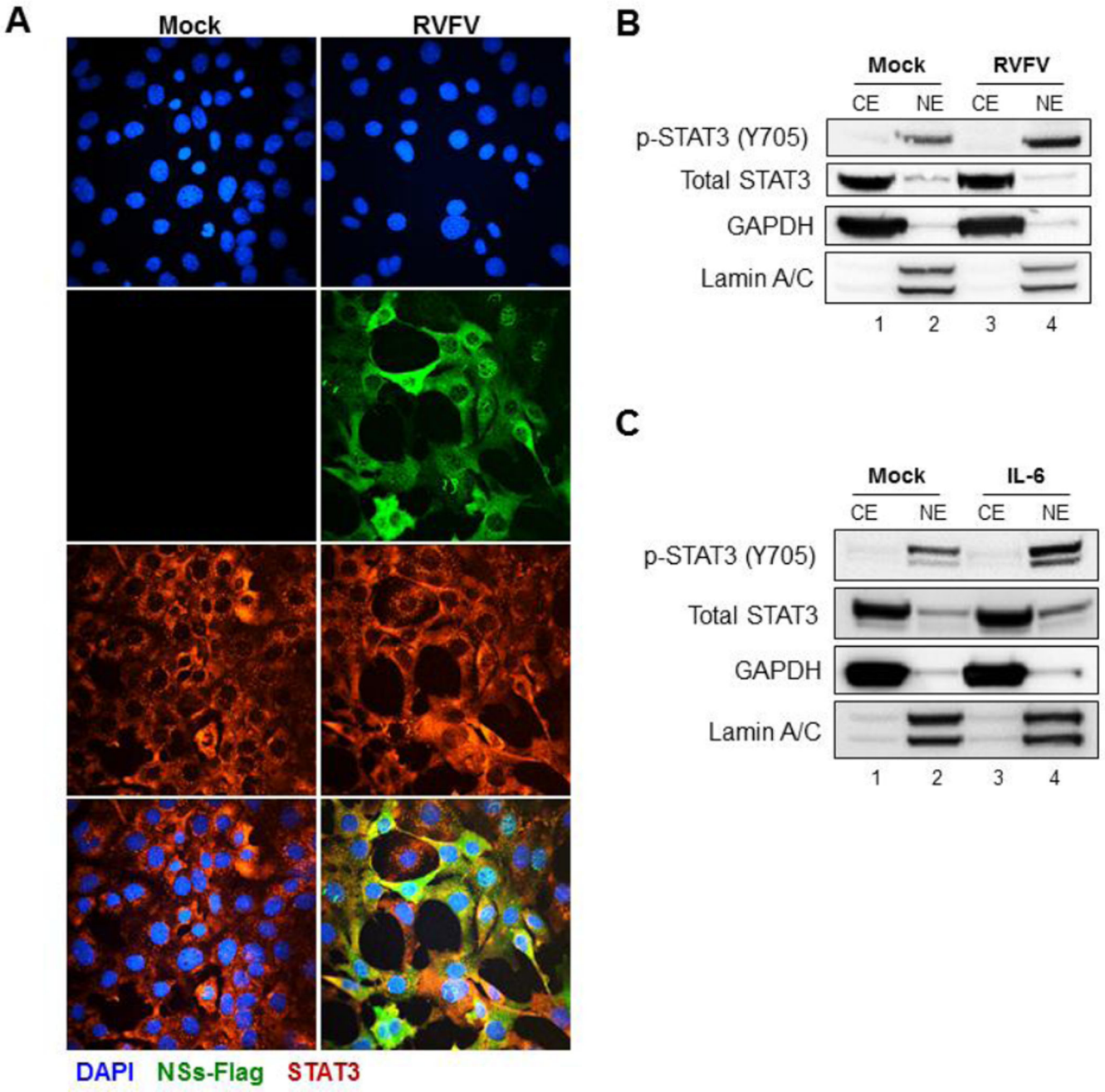

Figure 2. STAT3 localization in RVFV infected cells

A) MEFs were mock-infected or infected with MP12- NSs-Flag for one hour. Cells were fixed with 4% paraformaldehyde at 16 hpi and stained. Slides were probed for total STAT3 and an Alexa Fluor 568 labeled secondary antibody. As a positive control, cells were also probed for NSs (Flag-tag) and an Alexa Fluor 488 labeled secondary antibody. DAPI stain was used to visualize nuclei. Representative pictures of each sample from multiple experiments are shown. B) MEFs were mock-infected or infected with MP12 for one hour. Cells were collected at 16 hpi and cellular fractionation was performed. Cytoplasmic (CE) and nuclear (NE) extracts were separated by SDS-PAGE and analyzed by western blot.

Membranes were probed for p-STAT3 (Y705), total STAT3, GAPDH as a cytoplasmic control, and Lamin A/C as the nuclear control. C) MEFs were mock-treated or treated with 100 ng/mL of human IL-6 for 4 hours. Following treatment, cells were processed as described in panel B.

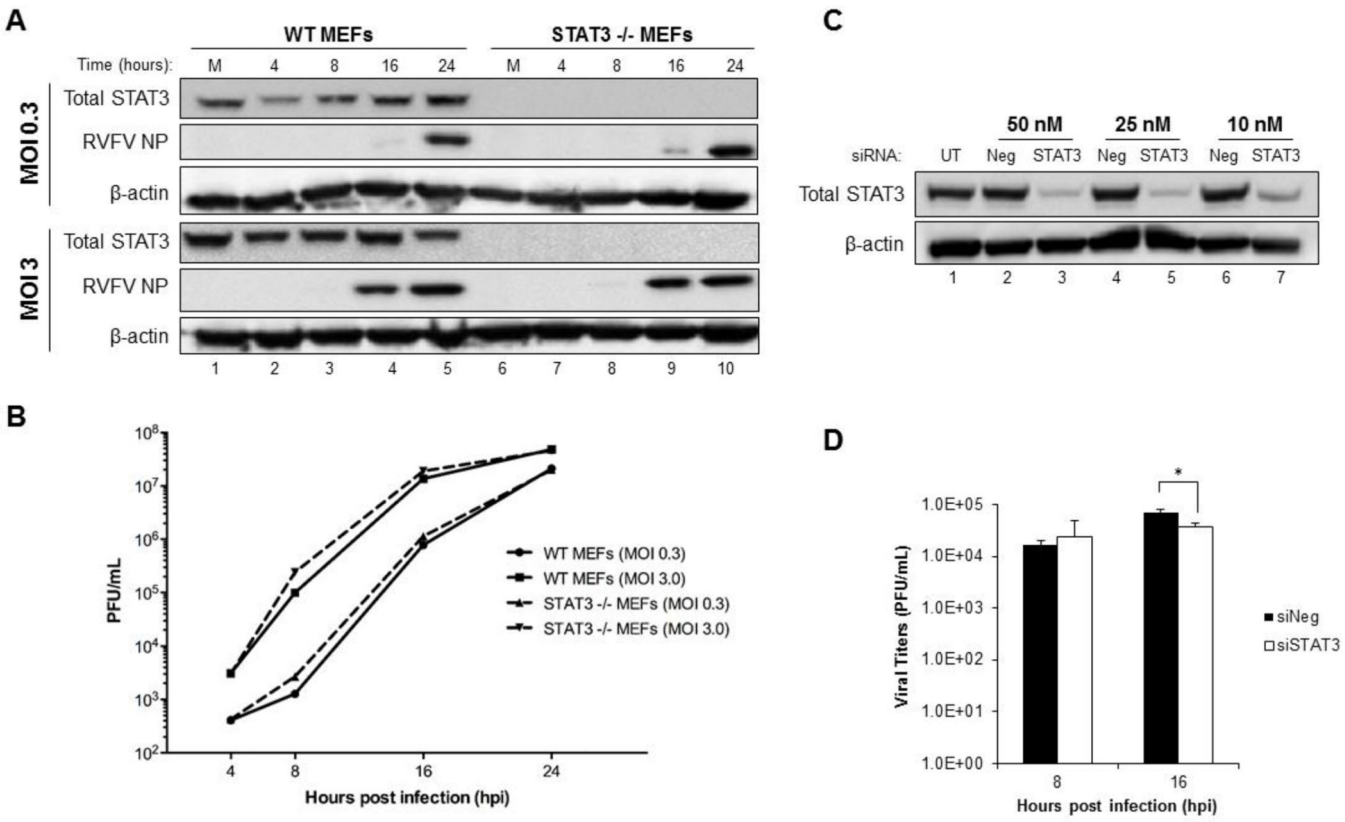

Figure 3. Loss of STAT3 does not alter RVFV replication kinetics

A) WT and STAT3−/− MEFs were mock-infected or infected with MP12 for one hour at MOI 0.3 or MOI 3.0. Cell lysates were collected at 4, 8, 16, and 24 hpi and analyzed by western blot. Membranes were probed for total STAT3, RVFV nucleoprotein (NP), or β-actin as a loading control. B) Cells were infected as described in (A) and supernatants were collected at 4, 8, 16, and 24 hpi (MOI 0.3 and 3.0) and analyzed by plaque assay. C) HSAECs were transfected with 10 nM, 25 nM, or 50 nM of siRNA against STAT3 or a negative control siRNA. The following day, the media was changed in order to reduce cell toxicity. Cells were incubated for 48 hours, then protein lysates were collected and analyzed by western blot. Membranes were probed for total STAT3 and β-actin as a loading control. D) HSAECs were transfected with 25 nM of siRNA against STAT3 or a negative control siRNA. At 48 hours post transfection, cells were infected with MP12 at MOI 3 for one hour. Supernatants were collected 8 and 16 hpi (72 hours post transfection) and analyzed by plaque assay. * $p \leq 0.05$

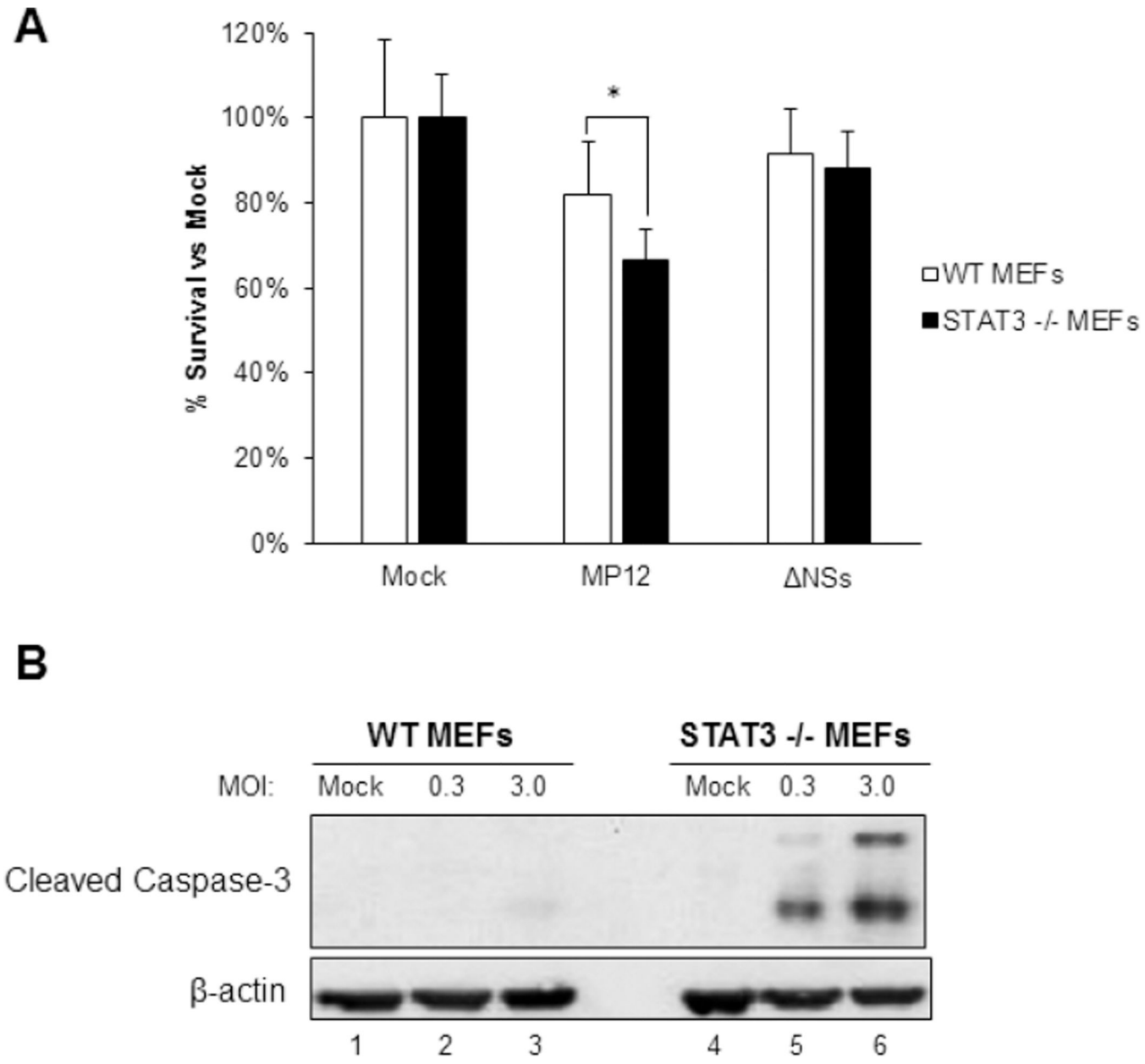

Figure 4. Loss of STAT3 increases RVFV-induced cell death

A) WT and STAT3−/− MEFs were mock-infected or infected with MP12 or MP12-ΔNSs for one hour at MOI 3.0. At 24 hpi, cell survival was analyzed using Promega's CellTiter-Glo Luminescent Cell Viability Assay according to the manufacturer's protocol. Cells were normalized to their corresponding mock sample. B) WT and STAT3 −/− MEFs were mock-infected or infected with MP12 for one hour at MOI 0.3 and 3. At 24 hpi, protein lysates were collected and analyzed by western blot. Membranes were probed using cleaved caspase-3 and β-actin as a loading control. * $p \leq 0.05$

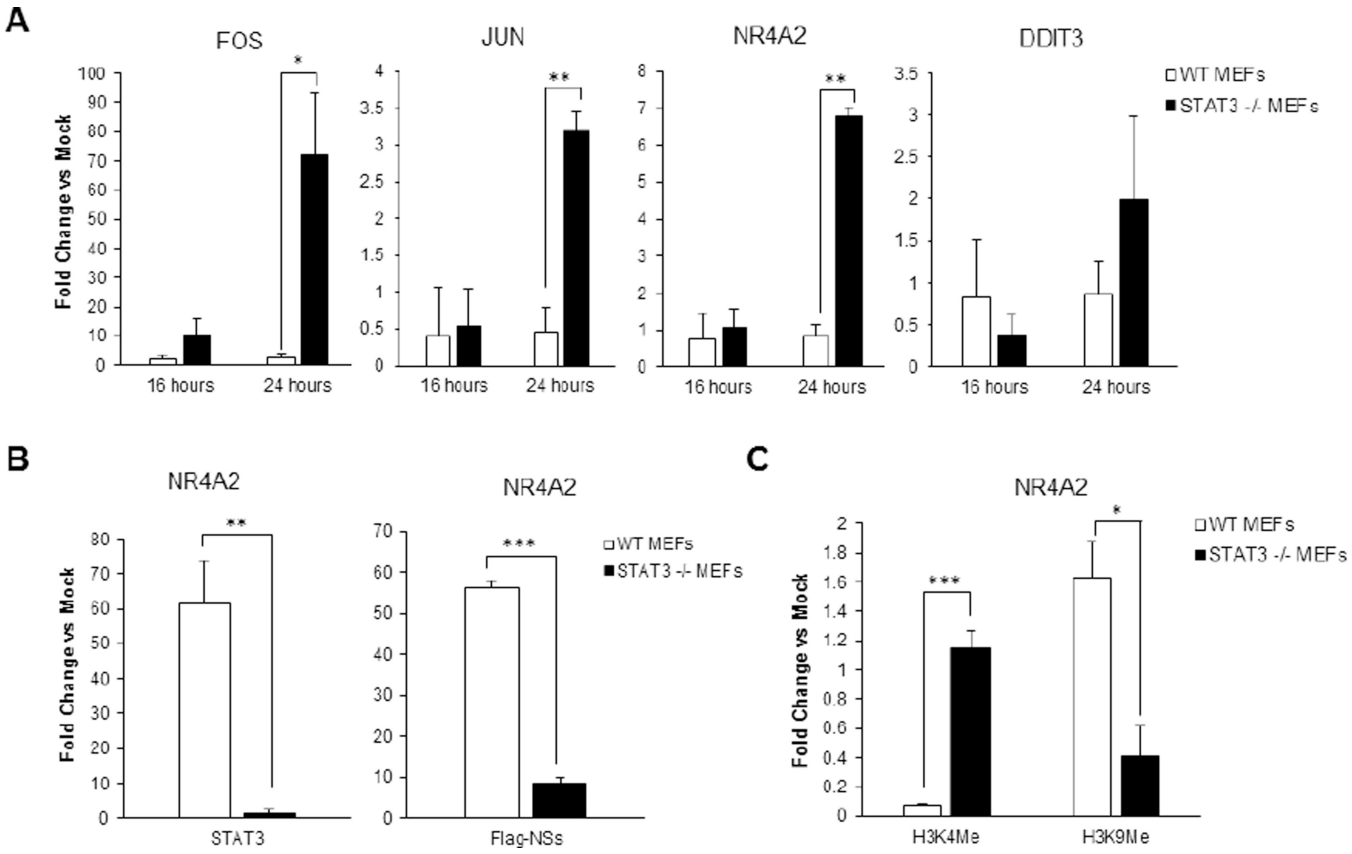

Figure 5. Loss of STAT3 leads to an increase in pro-apoptotic gene expression

A) WT and STAT3 −/− MEFs were mock-infected or infected with MP12 at MOI 3 for one hour. At 16 and 24 hpi, cells were lysed and RNA was collected using Qiagen's RNeasy Mini Kit according to manufacturer's instructions. Gene expression was analyzed by qRT-PCR using TaqMan Gene Expression Assays for *fos*, *jun*, *nr4a2 and ddit3*. Fold changes were calculated relative to 18S ribosomal RNA and normalized to mock samples using the ΔΔCt method. B) WT and STAT3 −/− MEFs were infected as described in (A) and fixed in 1% paraformaldehyde at 24 hpi. Samples were processed for ChIP analysis. Quantitative PCR was performed to analyze the presence of STAT3 and RVFV NSs at the *nr4a2* promoter. C) The same methods were used as in panel (B), using qPCR to analyze the presence of methylated histones H3K4Me3 and H3K9Me3 at the promoter of *nr4a2*. * $p \leq 0.05$, ** $p \leq 0.005$, *** $p \leq 0.0001$

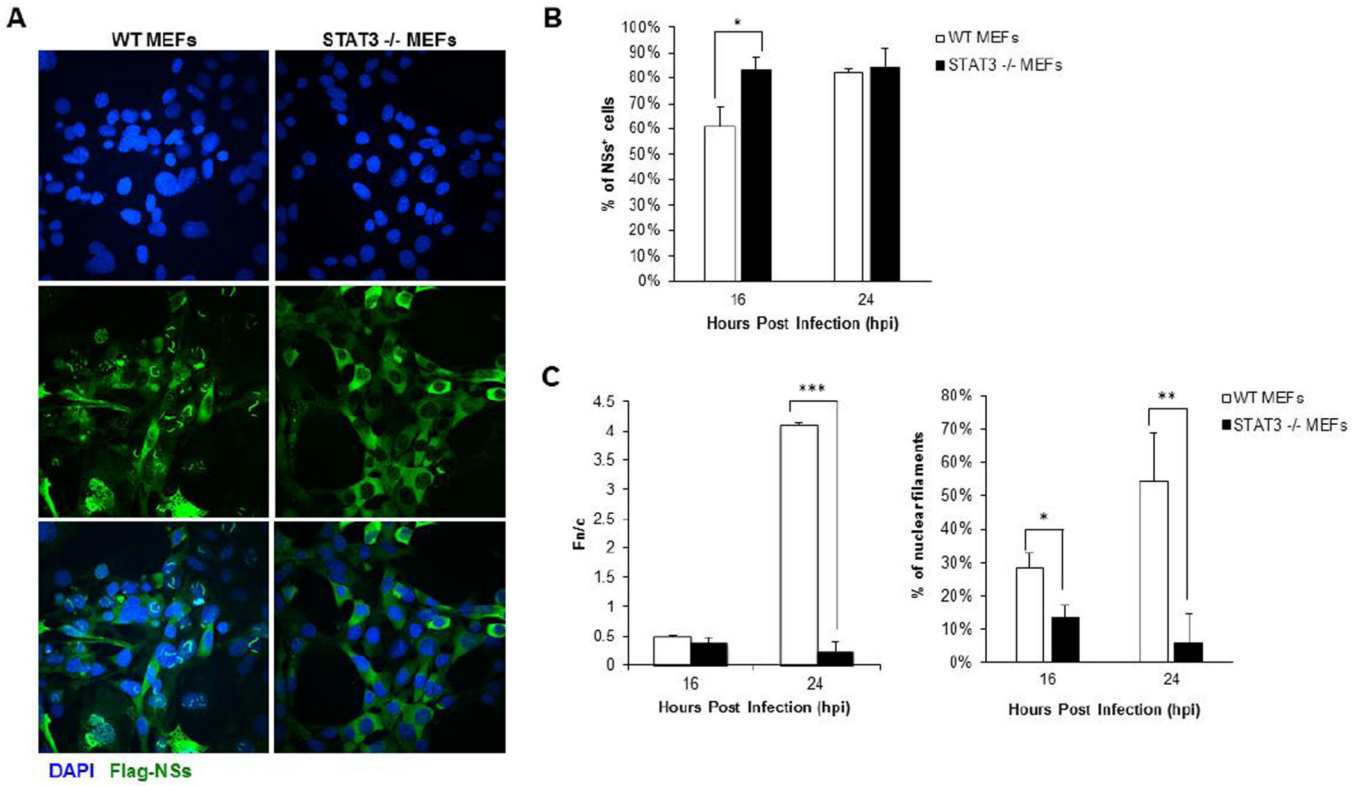

Figure 6. Lack of STAT3 causes a marked decrease in NSs filament formation

A) WT and STAT3 −/− MEFs were mock-infected or infected with MP12-NSs-Flag for one hour. Cells were fixed with 4% paraformaldehyde at 24 hpi and stained. Slides were probed for NSs (Flag-tag) and an Alexa Fluor 488 labeled secondary antibody. DAPI stain was used to visualize nuclei. Representative pictures of each sample from multiple experiments are shown. B) Digitalized images were processed as described in panel A, then at least 100 cells were analyzed for the presence of infection (NSs) for each sample. C) The same images were analyzed using the ImageJ version 1.47 public domain software (NIH) to determine the ratio of nuclear (Fn) to cytoplasmic (Fc) fluorescence (Fn/c). The same images were also analyzed for the presence of nuclear filaments for each sample. * $p \leq 0.05$, ** $p \leq 0.01$, *** $p \leq 0.0001$